HHS Public Access

Author manuscript

Cancer Immunol Res. Author manuscript; available in PMC 2020 March 04.

Published in final edited form as:

Cancer Immunol Res. 2017 February ; 5(2): 100–105. doi:10.1158/2326-6066.CIR-16-0223.

Metastatic Melanoma Patient Had a Complete Response with Clonal Expansion after Whole Brain Radiation and PD-1 Blockade

Cara L. Haymaker[1], **DaeWon Kim**[1], **Marc Uemura**[1], **Luis M. Vence**[2], **Ann Phillip**[1], **Natalie McQuail**[1], **Paul D. Brown**[3], **Irina Fernandez**[2], **Courtney W. Hudgens**[4], **Caitlin Creasy**[1], **Wen-Jen Hwu**[1], **Padmanee Sharma**[2], **Michael T. Tetzlaff**[4,5], **James P. Allison**[2], **Patrick Hwu**[1], **Chantale Bernatchez**[1], **Adi Diab**[1]

[1]Department of Melanoma Medical Oncology, The University of Texas MD Anderson Cancer Center, Houston, Texas.

[2]Department of Immunology, The University of Texas MD Anderson Cancer Center, Houston, Texas.

[3]Department of Radiation Oncology, The University of Texas MD Anderson Cancer Center, Houston, Texas.

[4]Department of Translational and Molecular Pathology, The University of Texas MD Anderson Cancer Center, Houston, Texas.

[5]Department of Pathology, The University of Texas MD Anderson Cancer Center, Houston, Texas.

Abstract

We report here on a patient with metastatic melanoma who had extensive brain metastases. After being treated with the sequential combination of whole brain radiation therapy followed by the PD-1–inhibitory antibody, pembrolizumab, the patient had a durable complete response. Retrospective laboratory studies of T cells revealed that, after treatment with anti-PD-1 commenced, effector $CD8^+$T cells in the blood expanded and the ratio of $CD8^+$:Treg T cells increased. A $CD8^+$ T-cell clone present in the initial brain metastases was expanded in the blood after anti-PD-1 treatment, which suggested an antitumor role for this clone. Immunohistochemical

Corresponding Authors: Adi Diab, The University of Texas MD Anderson Cancer Center, 1515 Holcombe Blvd., Houston, TX 77030. Phone: 713-745-7336; Fax: 713-745-1046; adiab@mdanderson.org; and Chantale Bernatchez, cbernatchez@mdanderson.org.

Authors' Contributions

Conception and design: P. Hwu, A. Diab

Development of methodology: M.T. Tetzlaff

Acquisition of data (provided animals, acquired and managed patients, provided facilities, etc.): D. Kim, L.M. Vence, A. Phillip, N. McQuail, C. Creasy, W.-J. Hwu, M.T. Tetzlaff, C. Bernatchez, A. Diab

Analysis and interpretation of data (e.g., statistical analysis, biostatistics, computational analysis): C.L. Haymaker, D. Kim, L.M. Vence, P.D. Brown, I. Fernandez, C.W. Hudgens, W.-J. Hwu, P. Sharma, M.T. Tetzlaff, P. Hwu, C. Bernatchez, A. Diab

Writing, review, and/or revision of the manuscript: C.L. Haymaker, D. Kim, M. Uemura, P.D. Brown, W.-J. Hwu, P. Sharma, M.T. Tetzlaff, P. Hwu, C. Bernatchez, A. Diab, J.P. Allison

Administrative, technical, or material support (i.e., reporting or organizing data, constructing databases): M.T. Tetzlaff, C. Bernatchez

Study supervision: A. Diab

Disclosure of Potential Conflicts of Interest

P. Sharma is a consultant/advisory board member for BMS. M.T. Tetzlaff is a consultant/advisory board member for Myriad Genetics and Seattle Genetics. No potential conflicts of interest were disclosed by the other authors.

analysis confirmed the presence of $CD8^+$ T cells and low PD-L1 expression in the brain metastases before immunotherapy initiation. This sequence of therapy may provide an option for melanoma patients with unresponsive brain metastases.

Introduction

Melanoma is the third most common solid tumor to metastasize to the brain (1, 2). Approximately 40% to 50% of patients with advanced melanoma develop brain metastases (3, 4), and brain metastases are found in up to 70% of patients upon autopsy (4, 5). The development of brain metastasis is one of the most common and devastating complications and is associated with poor prognosis and a median overall survival (OS) of 4 to 5 months (3, 6, 7). Radiotherapy approaches, such as whole brain radiation therapy (WBRT) and stereotactic radiosurgery (SRS), remain the cornerstone of management of brain metastases for most patients, due to poor responses to current systemic treatment, which is partially explained by the presence of the blood–brain barrier. Although surgical resection and SRS have shown high local control rates in selected patients who have good performance status, well-controlled extracranial disease, and a small number of brain lesions, WBRT remains the main treatment modality for patients with multiple brain lesions. WBRT can reverse acute neurologic deficits, provide symptomatic relief, and decrease intracranial relapse, but many tumors are or become refractory, which leads to challenging and morbid clinical situations. The clinical outcome for patients who require WBRT is poor, with a median OS of 3 to 4 months (6, 8, 9), which could be attributed to both worsening intracranial and systemic disease. Therefore, new effective therapeutic approaches are needed to improve clinical outcome of brain metastasis. BRAF inhibitors and ipilimumab now show promising clinical activities in brain metastases. However, BRAF inhibitors are effective only in patients with BRAF V600–mutant melanoma, who comprise approximately 50% of melanoma patients. Median progression-free survival (PFS) with BRAF inhibitor therapy is only 4 months in patients with metastatic brain disease, with a clinical response rate of 30% to 40% (10, 11). In contrast, ipilimumab has shown a clinical response rate of only 5% to 10% in metastatic brain disease (12). Recently, pembrolizumab (anti-PD-1) was approved for advanced melanoma and has shown better clinical response rate, PFS, OS, and toxicity profile than ipilimumab (13). However, data about clinical activity of pembrolizumab in metastatic brain disease are limited. Here, we report a patient with extensive brain metastatic disease who experienced a durable complete clinical response following sequential treatment of WBRT and pembrolizumab. CDR3 sequencing of the T cells present in the brain metastases and in the blood revealed the expansion of a unique $CD8^+$ T-cell clone during tumor regression. Overall, this combination appears therapeutic for patients with metastatic brain disease by providing access to the tumor site and reactivation of the antitumor immune response.

Materials and Methods

Flow cytometry

TILs were stained using Live/Dead Fixable Aqua Dead Cell Stain Kit (Life Technologies) according to the manufacturer’s instructions. Cells were stained with a combination of antibodies from BD Biosciences (unless indicated otherwise), including CD3 FITC (SK7),

CD4 PerCP-Cy5.5 (RPT-T4), CD8 PB (RPT-T8), 41BB (4B4–1), PD-1 (EH12.2H7, BioLegend), CTLA-4 (BNI3), ICOS (ISA3, eBioscience), OX40 (ACT35), CD45RO (UCHL1, Biolegend), CD45RA (HI100, eBioscience), CD62L (DREG-56, eBioscience), CCR7 (G043H7, BioLegend), and Ki67 (B56). For all flow cytometry assays described, data were acquired using a Canto II cytometer (BD Biosciences) and analyzed using FlowJo software (Tree Star version 7.6.5).

Cell sorting

Bulk $CD4^+$ and $CD8^+$ T cells were sorted from peripheral blood mononuclear cells (PBMC) using an Aria II (BD Biosciences) cell sorter directly into media (RPMI1640 + 10% human serum). Only populations with a ≥ 95% post-sort purity were used for experiments. Immediately following sorting, cells were washed twice in chilled PBS and flash frozen for DNA extraction.

Tracking TCR clonotypes through CDR3 sequencing

DNA was extracted from formalin-fixed paraffin-embedded (FFPE) brain metastasis, sorted $CD4^+$and $CD8^+$ T cells, as well as bulk PBMCs. Total DNA was isolated using the Qiagen AllPrep Kit, and samples were shipped to Adaptive Biotechnologies for sequencing of the T-cell receptor Vβ CDR3 region using the immunoSEQ assay (14). All analysis was performed in-house.

IHC for PD-L1 and CD8 expression on brain metastasis

FFPE tissue sections (4 μm) were subjected to heat-mediated antigen retrieval with Epitope Retrieval 1 solution (pH6, Leica Biosystems) for 20 minutes, then stained with the Bond RX system (Leica Biosystems) using the standard protocol. The sections were incubated with anti-CD8 at 1:25 dilution (Thermo Scientific #MS-457) or anti-PD-L1 at 1:100 dilution (Cell Signaling Technology #13684S). Visualization was performed using the Bond Polymer Refine Detection Kit (Leica Biosystems) according to the manufacturer's instructions.

Patient tumor sample acquisition

Tumor samples were obtained from stage IIIc to stage IV melanoma patients undergoing surgery at The University of Texas MD Anderson Cancer Center (Houston, TX) according to an Institutional Review Board–approved protocol and patient consent (IRB# LAB00–063).

Results

Clinical evaluation

A 60-year-old otherwise healthy female was diagnosed with unknown primary metastatic melanoma in the subcutaneous adipose tissue of the right thigh in June 2012. She underwent wide local excision of the lesion and a sentinel node biopsy, which revealed no residual melanoma and negative sentinel nodes. PCR-based DNA sequencing analysis determined the tumor cells to be *BRAF* wild type. Subsequently, she began adjuvant high-dose IFNα treatment. However, after 2 weeks, the treatment was discontinued due to suicidal ideation. She was well until June 2013, when two new metastatic lesions were noticed in her right

cerebellum. The brain lesions were treated with SRS. Subsequently, she had symptomatic disease progression of her brain lesions and in November 2013 underwent a craniotomy with resection of the brain lesions. In March 2014, an MRI scan of the brain revealed a new lesion in the right cerebellum without symptoms, for which she received 4 doses of ipilimumab (3 mg/kg). Upon repeat MRI in June 2014, further progression of previous lesions and at least 17 new brain lesions were detected (Fig. 1, left). The largest brain lesion measured 2.4 cm in its greatest dimension with multiple additional lesions ranging in greatest dimension from 3 to 7 mm. Subsequently, she was treated with WBRT of 30 Gy in 10 fractions and rapid tapering of dexamethasone treatment, which was completed within 10 days. In July of 2014, a post-WBRT MRI study showed no new brain lesions, but the existing multiple tumors had not responded (Fig. 1, middle). Following WBRT, the patient was started on pembrolizumab (2 mg/kg) every 3 weeks. Six weeks after starting pembrolizumab and 8 weeks after completing WBRT, a repeat MRI of the brain showed complete resolution of most of the brain lesions, with the exception of two enlarged lesions with hemorrhagic components, which we interpreted as treatment-related changes. These two lesions improved significantly after four more doses of pembrolizumab and completely resolved after a total of 10 doses (Fig. 1, right). Currently, 29 months after her first dose of pembrolizumab, the patient remains alive with no evidence of systemic or intracranial disease. Clinically, her performance status is excellent, with major complaints being low-grade fatigue and short-term memory loss.

Activation of effector CD8$^+$ T cells following WBRT and pembrolizumab

Given the complete resolution of disease, we retrospectively examined T-cell subsets in the peripheral blood collected over the course of the sequential therapy of ipilimumab → WBRT → pembrolizumab by flow cytometry. Blood was collected beginning with the second cycle of ipilimumab, with the last sample collected just prior to the patient's complete response (collections relative to treatments are shown in Fig. 2A). CD4$^+$ and CD8$^+$ T-cell proliferation, as well as expression of inhibitory markers, activation markers, differentiation status, and CD8$^+$:Treg ratio were examined. Consistent with previous findings from Wang and colleagues, the percentage of Ki67-positive cells within both the CD4$^+$ and CD8$^+$ T-cell pool increased during treatment with ipilimumab (Fig. 2B; ref. 15). In addition, the expression of ICOS on both the CD4$^+$ and CD8$^+$ T-cell subsets was increasing during ipilimumab therapy as has been previously reported (Fig. 2C and D; refs. 15, 16). After WBRT and subsequent anti-PD-1 therapy, the percentage of proliferating CD4$^+$ and CD8$^+$T cells first peaked briefly, then dropped to minimal levels (Fig. 2B). In addition, the expression of ICOS was also downregulated on both the subsets following initiation of anti-PD-1 (Fig. 2C and D). However, the percentages of both CD4$^+$CTLA-4$^+$ and CD8$^+$CTLA-4$^+$ T cells increased in blood early after initiation of pembrolizumab, which was followed by increased expression of PD-1 by both T-cell subsets. This suggests activation of a subset of both CD4$^+$ and CD8$^+$ T cells after sequential WBRT and pembrolizumab. Following WBRT (time point 4), an increase in the terminally differentiated effector CD8$^+$ T cells (T_{EMRA}) was observed and was maintained across time points 5 to 9, as the tumors regressed (Fig. 2E). The ratio of CD8:Treg (Fig. 2F) as well as CD8:CD4 (non-Tregs, Fig. 2G) was also increased during pembrolizumab therapy. Overall, WBRT followed by pembrolizumab resulted in the activation of both CD4$^+$ and CD8$^+$ T cells, an

increase in the numbers of effector $CD8^+$ T cells, and an increased CD8:Treg ratio in the blood, during which time the patient was responding to therapy.

Tracking intratumoral T cells present in the brain metastasis in response to pembrolizumab

The above assays are based on the assumption that changes in T-cell activation/differentiation and subsequent antitumor responses may be observed in the blood. However, this type of analysis does not provide insight into the presence of an initial immune response at the site of disease, nor does it allow for a defined tracking of the impact of these immunotherapy regimens on those T cells. In the case of this patient, only one biopsy was done on the brain metastases prior to the induction of ipilimumab (Fig. 2A, schematic, craniotomy). Immunohistochemical analyses confirmed the presence of $CD8^+$ tumor-infiltrating lymphocytes (TIL) at the tumor periphery that correlated with PD-L1 expression mostly in the stromal cells at the same site (Fig. 3A), demonstrating potential suppression of the $CD8^+$ immune response. To determine the impact of the immunotherapy regimen on the expansion and/or contraction of $CD8^+$ TILs, we utilized high-throughput CDR3 sequencing. We compared the CDR3 sequences from intratumoral T cells present in the brain metastasis with those in circulating peripheral blood T cells collected during subsequent ipilimumab therapy and at the time of complete response to WBRT + pembrolizumab. $CD3^+CD4^+$ and $CD3^+CD8^+$ T-cell subsets were sorted from the last PBMC time point to backtrack these T-cell subsets through time in the blood, as well as to determine their presence in the brain metastases. Sequencing of the TILs in the brain showed a higher frequency of $CD8^+$ T cells, compared with $CD4^+$ T cells ($P < 0.0001$, Fig. 3B). The $CD8^+$ T-cell clones found in the brain metastasis were then assessed in the blood. The frequency of these clones did not significantly increase between ipilimumab cycle 3 and pembrolizumab cycle 11 ($P = 0.114$, Fig. 3C). However, analysis of the top 100 $CD8^+$ T-cell clones present in the circulation showed a significant expansion after pembrolizumab ($P = 0.0241$, Fig. 3D). The $CD8^+$ T-cell clone with the highest frequency in the blood was also found in the brain metastases and had expanded following pembrolizumab. This $CD8^+$ T-cell clone was the dominant clone found in the tumor site (frequency of 17.2%, dark red color, Fig. 3B), suggesting an antitumor response that was unable to clear the tumor. There was also no change in the frequency of the top 100 $CD4^+$ T cells at the time points examined ($P = 0.9202$, Fig. 3E). Overall, this type of analysis demonstrates that a $CD8^+$ T-cell response was present in the brain metastases prior to initiation of immunotherapy and was subjected to inhibition by the local tumor microenvironment via the PD-1/PD-L1 axis. In addition, although WBRT + pembrolizumab did not appear to have an impact on the clonal expansion of $CD4^+$ T cells, a significant expansion was observed from the $CD8^+$ T-cell subset.

Discussion

In this case report, we observed the presence of $CD8^+$ T cells in the brain metastases prior to initiation of immunotherapy. These T cells were localized to an area where PD-L1 expression was detected, which suggested that an immune response was present and yet being suppressed by the tumor microenvironment, likely through the PD-1/PD-L1 axis. This also provides a rationale for the positive response to pembrolizumab, as response to anti-

PD-1 has been demonstrated to be associated with the presence of PD-L1 (13, 17, 18). Although ipilimumab does not cross the blood–brain barrier, the combination of ipilimumab and SRS can increase OS in patients with multiple brain metastases (19). In our patient, the activation of T cells in the circulation following ipilimumab therapy, but the lack of clinical response in the brain, may have been due to an immune escape mechanism other than CTLA-4 signaling. Another explanation for the lack of response could have been the lack of sufficient $CD8^+$ T-cell infiltration into the tumor site (CNS). Although no PBMC samples were available pre-ipilimumab treatment, we cannot discount the possibility that ipilimumab may have primed an immune response that was subsequently observed by the combination of WBRT and anti-PD-1. Although one mode of action of ipilimumab is to bring in new T-cell clones into the tumor, an influx of newly activated cells perhaps was blocked in this patient, due to the absence of adhesion molecules at the blood–brain barrier.

Instead, the mechanism of action may be due to the combination of WBRT and anti-PD-1. WBRT enhances antitumor immunity not only by activation of DCs, but also by upregulation of adhesion molecules, such as ICAM and VCAM in the blood–brain barrier (20, 21). Anti-PD-1 treatment, on the other hand, increases the frequency of effector T cells (Fig. 2E) that are known to have high expression of adhesion molecules ligands, such integrins, which would in turn enhance their infiltration into brain lesions while providing for a reactivation of the T cells already present at the tumor site (22). Although the posttherapy biopsies do not definitively prove this mode of response, analysis of the $CD8^+$ T-cell response following anti-PD-1 by CDR3 sequencing does demonstrate expansion of a subset of $CD8^+$ T cells present in the metastases prior to immunotherapy following WBRT + pembrolizumab. This analysis identified the presence of a dominant $CD8^+$ T-cell clone in the brain that had the highest frequency and expanded in the blood following pembrolizumab. No such clone was observed in the $CD4^+$ T-cell subset. Given the activated state of the $CD8^+$ T cells in the blood following WBRT + pembrolizumab (i.e., upregulation of 41BB followed by expression of PD-1), the increased adhesion molecules present at the blood–brain barrier due to WBRT would have allowed these activated T cells to gain entry and mediate an additional antitumor effect. The combination of radiotherapy and immunotherapy can elicit synergistic antitumor responses (23). Although several clinical trials are testing various combinations, these data emphasize another mechanism of synergy unique to anti-PD-1 and WBRT for patients with brain metastases.

Overall, this case report provides a rationale for the treatment of metastatic melanoma patients with brain metastases with combination of WBRT + anti-PD-1 (1). A larger study using this combination therapy may provide the data to support this as an effective treatment option for patients with unresponsive brain metastases in not only melanoma, but in lung cancer and other cancers where anti-PD-1 as also been approved.

Acknowledgments

The authors would like to thank the MDACC Immunotherapy Platform for performing the PBMC processing and staining. The authors would also like to thank the MDACC Melcore for the banking of biopsy specimens and FFPE tissue cutting and slide preparation.

References

1. Schouten LJ, Rutten J, Huveneers HA, Twijnstra A. Incidence of brain metastases in a cohort of patients with carcinoma of the breast, colon, kidney, and lung and melanoma. Cancer 2002;94:2698–705. [PubMed: 12173339]
2. Barnholtz-Sloan JS, Sloan AE, Davis FG, Vigneau FD, Lai P, Sawaya RE. Incidence proportions of brain metastases in patients diagnosed (1973 to 2001) in the metropolitan detroit cancer surveillance system. J Clin Oncol 2004;22:2865–72. [PubMed: 15254054]
3. Davies MA, Liu P, McIntyre S, Kim KB, Papadopoulos N, Hwu WJ, et al. Prognostic factors for survival in melanoma patients with brain metastases. Cancer 2011;117:1687–96. [PubMed: 20960525]
4. Amer MH, Al-Sarraf M, Baker LH, Vaitkevicius VK. Malignant melanoma and central nervous system metastases: incidence, diagnosis, treatment and survival. Cancer 1978;42:660–8. [PubMed: 679158]
5. de la Monte SM, Moore GW, Hutchins GM. Patterned distribution of metastases from malignant melanoma in humans. Cancer Res 1983;43:3427–33. [PubMed: 6850649]
6. Raizer JJ, Hwu WJ, Panageas KS, Wilton A, Baldwin DE, Bailey E, et al. Brain and leptomeningeal metastases from cutaneous melanoma: survival outcomes based on clinical features. Neuro Oncol 2008;10:199–207. [PubMed: 18287337]
7. Fife KM, Colman MH, Stevens GN, Firth IC, Moon D, Shannon KF, et al. Determinants of outcome in melanoma patients with cerebral metastases. J Clin Oncol 2004;22:1293–300. [PubMed: 15051777]
8. de la Fuente M, Beal K, Carvajal R, Kaley TJ. Whole-brain radiotherapy in patients with brain metastases from melanoma. CNS Oncol 2014;3:401–6. [PubMed: 25438811]
9. Hauswald H, Dittmar JO, Habermehl D, Rieken S, Sterzing F, Debus J, et al. Efficacy and toxicity of whole brain radiotherapy in patients with multiple cerebral metastases from malignant melanoma. Radiat Oncol 2012;7:130. [PubMed: 22857154]
10. Long GV, Trefzer U, Davies MA, Kefford RF, Ascierto PA, Chapman PB, et al. Dabrafenib in patients with Val600Glu or Val600Lys BRAF-mutant melanoma metastatic to the brain (BREAK-MB): a multicentre, open-label, phase 2 trial. Lancet Oncol 2012;13:1087–95. [PubMed: 23051966]
11. Dummer R, Goldinger SM, Turtschi CP, Eggmann NB, Michielin O, Mitchell L, et al. Vemurafenib in patients with BRAF (V600) mutation-positive melanoma with symptomatic brain metastases: final results of an open-label pilot study. Eur J Cancer 2014;50:611–21. [PubMed: 24295639]
12. Margolin K, Ernstoff MS, Hamid O, Lawrence D, McDermott D, Puzanov I, et al. Ipilimumab in patients with melanoma and brain metastases: an open-label, phase 2 trial. Lancet Oncol 2012;13:459–65. [PubMed: 22456429]
13. Robert C, Schachter J, Long GV, Arance A, Grob JJ, Mortier L, et al. Pembrolizumab versus ipilimumab in advanced melanoma. N Engl J Med 2015;372:2521–32. [PubMed: 25891173]
14. Robins HS, Campregher PV, Srivastava SK, Wacher A, Turtle CJ, Kahsai O, et al. Comprehensive assessment of T-cell receptor beta-chain diversity in alphabeta T cells. Blood 2009;114:4099–107. [PubMed: 19706884]
15. Wang W, Yu D, Sarnaik AA, Yu B, Hall M, Morelli D, et al. Biomarkers on melanoma patient T cells associated with ipilimumab treatment. J Transl Med 2012;10:146. [PubMed: 22788688]
16. Fu T, He Q, Sharma P. The ICOS/ICOSL pathway is required for optimal antitumor responses mediated by anti-CTLA-4 therapy. Cancer Res 2011;71:5445–54. [PubMed: 21708958]
17. Topalian SL, Hodi FS, Brahmer JR, Gettinger SN, Smith DC, McDermott DF, et al. Safety, activity, and immune correlates of anti-PD-1 antibody in cancer. N Engl J Med 2012;366:2443–54. [PubMed: 22658127]
18. Larkin J, Chiarion-Sileni V, Gonzalez R, Grob JJ, Cowey CL, Lao CD, et al. Combined nivolumab and ipilimumab or monotherapy in untreated melanoma. N Engl J Med 2015;373:23–34. [PubMed: 26027431]

19. Knisely JP, Yu JB, Flanigan J, Sznol M, Kluger HM, Chiang VL. Radiosurgery for melanoma brain metastases in the ipilimumab era and the possibility of longer survival. J Neurosurg 2012;117:227–33. [PubMed: 22702482]

20. Lee WH, Sonntag WE, Lee YW. Aging attenuates radiation-induced expression of pro-inflammatory mediators in rat brain. Neurosci Lett 2010;476:89–93. [PubMed: 20385203]

21. Shulman Z, Cohen SJ, Roediger B, Kalchenko V, Jain R, Grabovsky V, et al. Transendothelial migration of lymphocytes mediated by intraendothelial vesicle stores rather than by extracellular chemokine depots. Nat Immunol 2012;13:67–76.

22. Peng W, Liu C, Xu C, Lou Y, Chen J, Yang Y, et al. PD-1 blockade enhances T-cell migration to tumors by elevating IFN-gamma inducible chemokines. Cancer Res 2012;72:5209–18. [PubMed: 22915761]

23. Diab A, Jenq RR, Rizzuto GA, Cohen AD, Huggins DW, Merghoub T, et al. Enhanced responses to tumor immunization following total body irradiation are time-dependent. PLoS One 2013;8:e82496. [PubMed: 24349298]

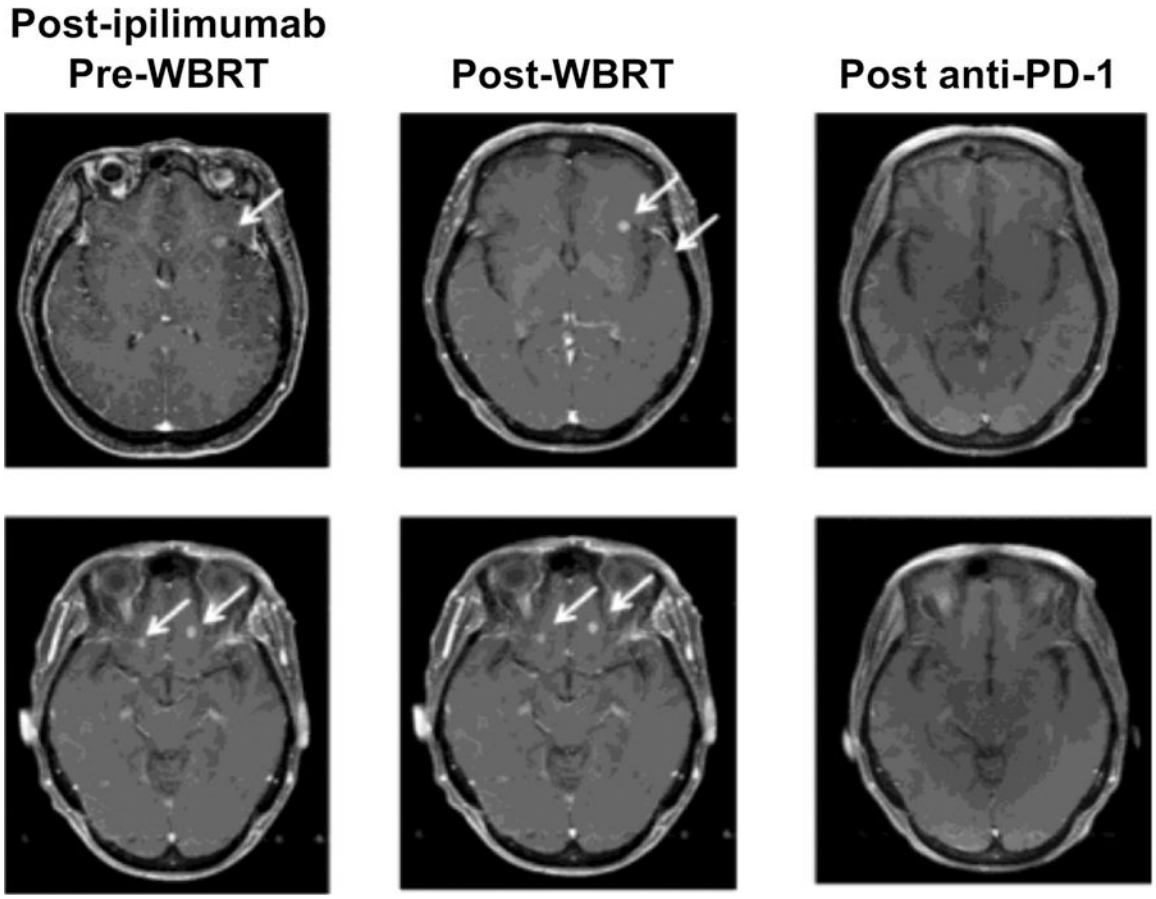

Figure 1.

Imaging of brain metastases over the course of therapy. MRI of the brain shows large numbers of brain metastases after ipilimumab therapy (left), which continued to be detectable after WBRT (middle). All detectable brain metastases resolved after anti-PD-1 therapy (right).

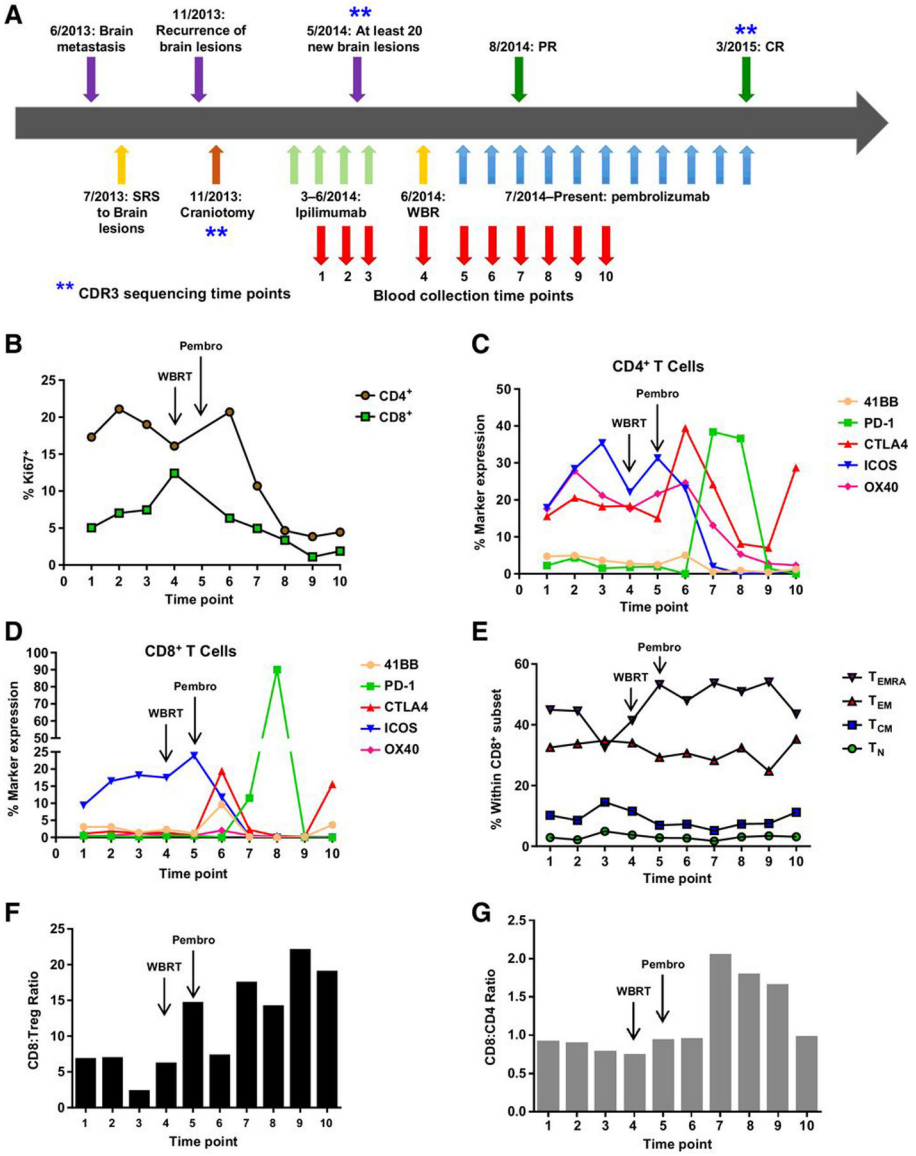

Figure 2.

Expansion of effector cells in the blood during pembrolizumab (Pembro) therapy. **A**, A schematic of lesion occurrences and therapies over time. **B-G**, PBMC samples were collected at multiple times as depicted and stained for multiple markers, including T-cell subset markers CD8, CD4, and FoxP3, as well as markers for T-cell differentiation (CD45RA, CD45RO, CCR7, and CD62L), activation and inhibition (41BB, PD-1, CTLA-4, ICOS, and OX40), and proliferation (Ki67) by flow cytometry. Live, single cells were gated first by excluding populations expressing CD14, CD16, CD19, CD20, CD56, CD303, and TCRγδ followed by gating on $CD3^+CD4^+CD8^-$ and $CD3^+CD4^-CD8^+$ subsets. **B**, The percentage of proliferating $CD4^+$ and $CD8^+$ T cells, by Ki67 expression. $CD4^+$ (**C**) and $CD8^+$ (**D**) T cells were assessed for levels of activation and inhibitory markers 41BB, PD-1, CTLA-4, ICOS, and OX40. The percent expression of these markers within the $CD4^+$ or $CD8^+$ T-cell subset was tracked over time in the blood during therapy. **E**, The differentiation

status of the $CD8^+$ T-cell pool tracked over time as a percentage within the $CD8^+$ subset with gating as follows (T_N, $CD62L^+CCR7^+CD45RA^+CD45RO^-$; T_{CM}, $CD62L^+CCR7^+CD45RA^-CD45RO^+$; T_{EM}, $CD62L^-CCR7^-CD45RA^-CD45RO^+$; T_{EMRA}, $CD62L^-CCR7^-CD45RA^+CD45RO^-$). **F**, The CD8:Treg ratio was determined by dividing the number $CD8^+$ T cells by the number of $CD4^+FoxP3^+$ T cells at the same time point. **G**, The CD8:CD4 ratio was determined by dividing the number $CD8^+$ T cells by the number of $CD4^+FoxP3^-$ T cells at the same time point.

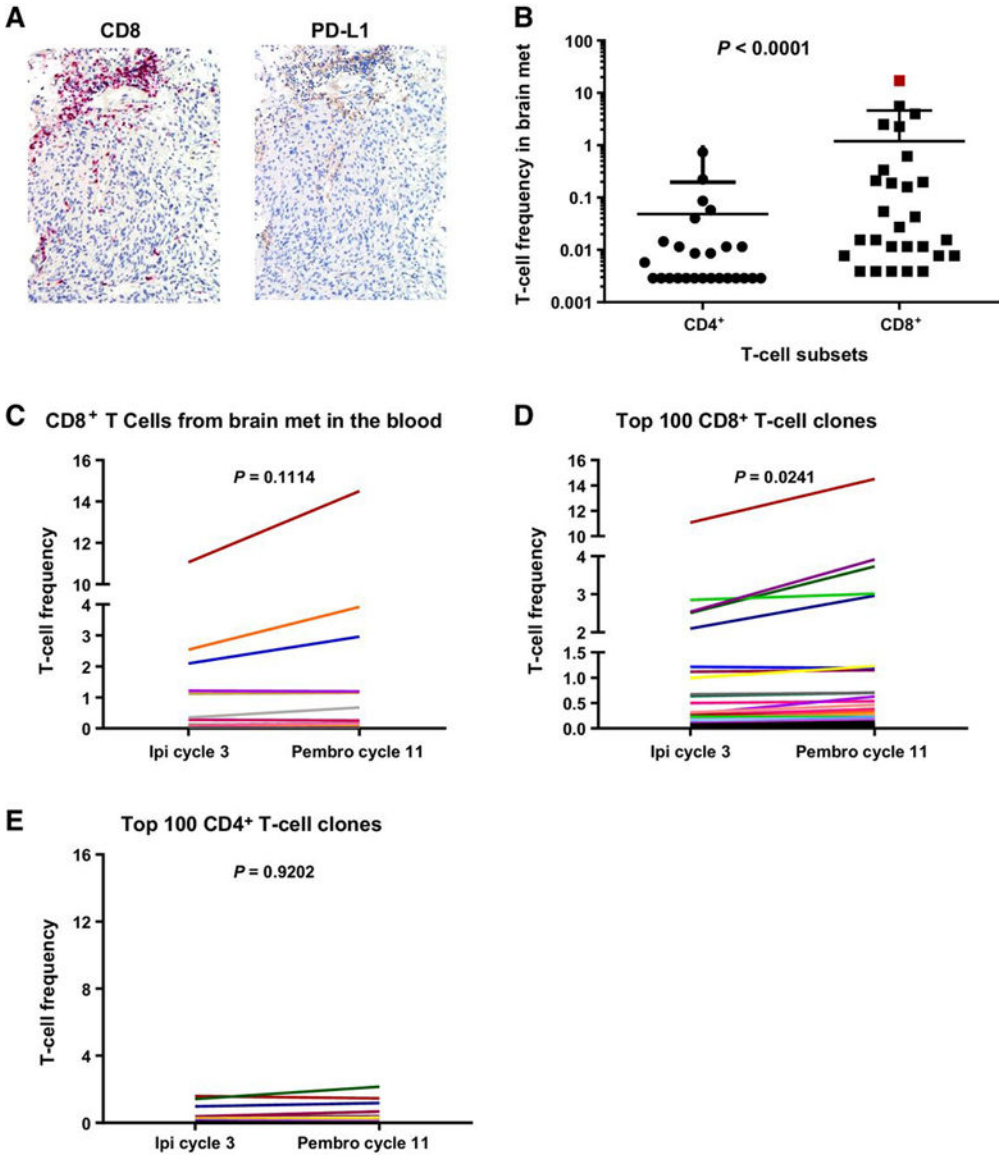

Figure 3.

Presence of immune infiltrate in brain metastases prior to immunotherapy and $CD8^+$ T-cell expansion following pembrolizumab (Pembro). **A**, Immunohistochemical staining for CD8 and PD-L1 of a brain metastasis present prior to immunotherapy initiation. **B-E**, CDR3 sequencing of DNA derived from the brain metastasis FFPE, sorted $CD3^+CD4^+$ and $CD3^+CD8^+$ T cells from PBMCs, and bulk PBMCs. The bulk PBMCs were collected from ipilimumab (Ipi) cycle 3 and pembrolizumab cycle 11. **B**, The frequency of $CD4^+$ and $CD8^+$ T-cell subset in the brain metastasis at the same time point as in **A**. **C**, $CD8^+$ T cell CDR3 sequences present in the brain metastasis were tracked in the blood at the two time points shown (ipilimumab cycle 3 and pembrolizumab cycle 11). **D**, The frequency of the top 100 $CD8^+$ T-cell clones (in terms of frequency) was assessed at the same time points. **E**, Frequency of the top 100 $CD4^+$ T cells clones across the two time points assessed.